IEEE Access
Multidisciplinary | Rapid Review | Open Access Journal

Date of publication xxxx 00, 0000, date of current version xxxx 00, 0000.

Digital Object Identifier 10.1109/ACCESS.20xx.DOI

Evaluation of Accelerometric and Cycling Cadence Data for Motion Monitoring

HANA CHARVÁTOVÁ[1], ALEŠ PROCHÁZKA[2,3,4], (Life Member, IEEE), OLDŘICH VYŠATA[4], (Member, IEEE), CARMEN PAZ SUÁREZ-ARAUJO[5], JONATHAN HURNDALL SMITH[6]

[1]Faculty of Applied Informatics, Tomas Bata University in Zlin, 760 01 Zlín, Czech Republic, e-mail: hcharvatova@email.cz
[2]Department of Computing and Control Engineering, University of Chemistry and Technology at Prague, 160 00 Prague, e-mail: A.Prochazka@ieee.org
[3]Czech Institute of Informatics, Robotics and Cybernetics, Czech Technical University of Prague, 160 00 Prague, Czech Republic
[4]Department of Neurology, Faculty of Medicine, Charles University at Hradec Králové, 500 05 Hradec Králové, Czech Republic, e-mail: vysatao@gmail.com
[5]Instituto Universitario de Ciencias y Tecnologías Cibernéticas, Universidad de Las Palmas de Gran Canaria, Las Palmas de Gran Canaria, Spain, e-mail: carmenpaz.suarez@ulpgc.es
[6]Bellford Consultancy Services Ltd., London, United Kingdom, e-mail: jonathan@bellford.co.uk

Corresponding author: H.Charvatova (e-mail: hcharvatova@email.cz).

The work has been supported by the research grant No. LTAIN19007 Development of Advanced Computational Algorithms for Evaluating Post-surgery Rehabilitation.

ABSTRACT Motion pattern analysis uses methods for the recognition of physical activities recorded by wearable sensors, video-cameras, and global navigation satellite systems. This paper presents the motion analysis during cycling, using data from a heart rate monitor, accelerometric signals recorded by a navigation system, and the sensors of a mobile phone. The set of real cycling experiments was recorded in a hilly area with each route about 12 km long. The associated signals were analyzed with appropriate computational tools to find the relationships between geographical and physiological data including the heart rate recovery delay studied as an indicator of physical and nervous condition. The proposed algorithms utilized methods of signal analysis and extraction of body motion features, which were used to study the correspondence of heart rate, route profile, cycling speed, and cycling cadence, both in the time and frequency domains. Data processing included the use of Kohonen networks and supervised two-layer softmax computational models for the classification of motion patterns. The results obtained point to a mean time of 22.7 s for a 50 % decrease of the heart rate after a heavy load detected by a cadence sensor. Further results point to a close correspondence between the signals recorded by the body worn accelerometers and the speed evaluated from the GNSSs data. The accuracy of the classification of downhill and uphill cycling based upon accelerometric data achieved 93.9 % and 95.0 % for the training and testing sets, respectively. The proposed methodology suggests that wearable sensors and artificial intelligence methods form efficient tools for motion monitoring in the assessment of the physiological condition during different sports activities including cycling, running, or skiing. The use of wearable sensors and the proposed methodology finds a wide range of applications in rehabilitation and the diagnostics of neurological disorders as well.

INDEX TERMS Multimodal signal analysis, computational intelligence, machine learning, motion monitoring, accelerometer-derived cycling data, classification.

I. INTRODUCTION

The discipline of motion recognition, using a range of measurement techniques to characterise the motion associated with different of physical activities, is an increasingly important topic. Applications include the assessment of rehabilitation exercises, gait analysis [1]–[4], breathing [5], detection of neurological disorders [6], the effect of cycling on cognitive functions [7], and the evaluation of fitness level in sports disciplines. Measurement techniques include the use of wearable sensors, smartphones, smartwatch-based

This article has been accepted for publication in a future issue of this journal, but has not been fully edited. Content may change prior to final publication. Citation information: DOI 10.1109/ACCESS.2021.3111323, IEEE Access

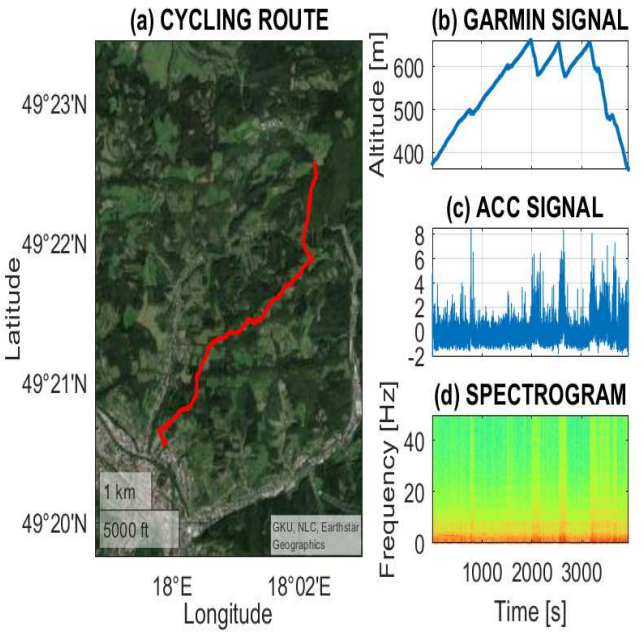

FIGURE 1. The area of cycling experiments presenting (a) the cycling route in the geographical environment, (b) the altitude GPS signal recorded by the Garmin system, (c) the accelerometric (ACC) signal recorded by the mobile sensor, and (d) spectrogram of a selected experiment.

biometrics [8], and computational intelligent methods for data processing.

Many motion tracking systems [9], [10] make use of global navigation satellite systems (GNSSs). They benefit from the increasing accuracy of GNSSs that are based on the use of new satellite systems, including Galileo [11] and the global positioning system (GPS). These systems may also be used for monitoring cycling routes [12]. Further commonly used sensors include accelerometers [13], [14] inside mobile phones [15], gyrometers, and sensors to monitor the heart rate [16] and further physiological functions. Mobile applications for smartphones can use these sensors, making them a viable alternative to bike computers [17]. Camera systems [18], [19] that use red-green-blue, depth and thermal sensors [20]–[22], and ultrasound systems [23] are very important as well. Associated studies include the assessment of road surface roughness [24] and three-dimensional modelling.

Separate accelerometers or their synchronized systems are used in many different applications, which employ standard or deep learning methods for classification of motion patterns. For example, these methods are used in the diagnosis of motion disorders in neurology and ataxic gait monitoring [25], [26]. Analysis of the sensor placement for the best separation ability is one of the fundamental problems of these studies. In addition, accelerometers have been used to evaluate motion symmetry [14] and to monitor rehabilitation exercises. These sensors are now included in most mobile phones and the possibility to use such wearable sensors enables the monitoring of different sport activities [27].

Appropriate methods of signal and image processing are then applied for information extraction. These methods include signal analysis in both spectral and scale domains, and modern methods that are based on wavelet transforms [28], artificial intelligence using machine learning, dimensionality reduction [29]–[31], classification methods, and deep convolutional neural networks.

The present paper is devoted to the analysis of data recorded during cycling [27], [32]–[35] in real conditions on the route presented in Fig. 1, which is located in a hilly area and is about 12 km long, and visualized in the Matlab environment using its mapping toolbox. Positioning data recorded by the GNSSs are synchronized with the heart rate and accelerometric data. The goal of this study is to show how wearable sensors can be used for post-exercise analysis of cycling-related information to detect the relationship between physiological data, accelerometric signals acquired at the specific body position, and the route profile recorded by the GNSSs. Our mathematical analysis is based on spectrograms using the Kohonen network learning system for data clustering and the two layer neural network for classification of accelerometric signals. Selected results are compared with those evaluated on a home exercise bike [36].

The research area includes a general methodology for multimodal data evaluation [37]–[39]. This points both to the rapid evolution of new engineering systems for data acquisition and to modern methods for signal processing, which will enable the application of deep learning, modelling of sophisticated structures, and the application of smart devices and assisted technologies in the future.

II. METHODS

A. DATA ACQUISITION

Fig. 1 presents the geographical data that were acquired by the GNSS and the associated accelerometric signals that were recorded by the mobile phone. The cycling route was located in a hilly area of Moravia close to Vsetin, and included segments with different surface qualities and occasional traffic that contributed to random errors in the recorded signals. The associated route profile with further Garmin and heart rate data are presented in Fig. 2 for a selected cycling experiment.

The cycling cadence-derived data [40] were used for segmentation of accelerometric and heart rate signals in different route areas.

The GNSS and motion data (time stamps, longitude, latitude, altitude, cycling distance, the speed, and the cycling cadence) were simultaneously recorded by a Garmin fitness watch (Fenix 5S). The heart rate data were acquired by a Garmin chest strap that was connected to a Garmin watch by ANT+ technology. All of the datasets were acquired during 26 cycling experiments in a hilly area on a route that is 12 km long, with an altitude difference of 300 m. Records were subsequently stored to the Garmin Connect website, exported as TCX files, converted to CSV files, and then imported to the MATLAB software for further processing.

This article has been accepted for publication in a future issue of this journal, but has not been fully edited. Content may change prior to final publication. Citation information: DOI 10.1109/ACCESS.2021.3111323, IEEE Access

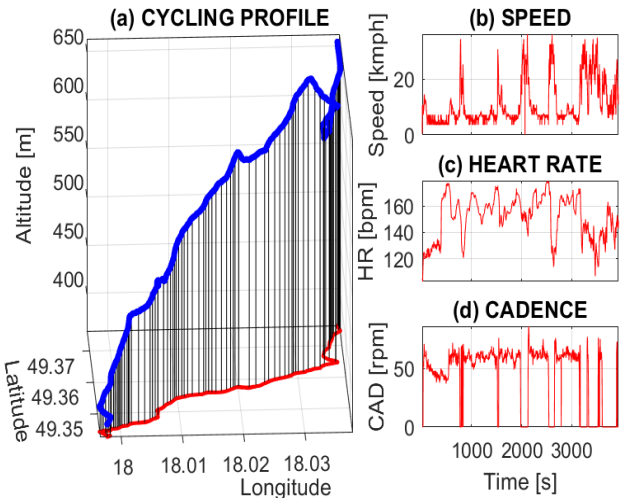

FIGURE 2. Signals recorded on the cycling route presenting (a) the cycling profile, (b) speed, (c) heart rate, and (d) the cadence recorded during a selected experiment.

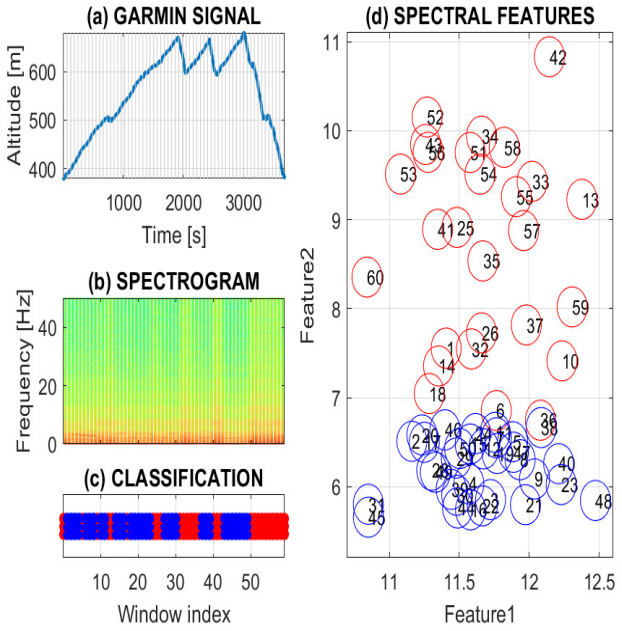

FIGURE 3. Feature extraction for (a) the cycling route recorded by the GNSS signal and divided into segments with a selected length of 60 s, (b) spectrogram of the accelerometric signal, (c,d) features specified into two selected spectral regions, and clustering results from the unsupervised Kohonen learning process.

Accelerometric data were recorded by the mobile phone in the spine position, which was selected following previous studies [25], [41], which described the higher discriminative abilities of sensors located in the upper half of the body [42], [43] in comparison to other positions. The sampling frequency of the Android mobile phone sensor was 100 Hz during all cycling routes.

All procedures involving human participants were in accordance with the ethical standards of the Institutional research committee and with the 1964 Helsinki Declaration and its later amendments.

B. SIGNAL PROCESSING

The proposed data evaluation method included a preprocessing stage. All sensors recorded both time stamps and observed values, but the sampling rate varied. This is the reason why resampling was necessary. The new sampling period T_s was selected as the average sampling period of the observed values and linear interpolation was then applied for their evaluation. In the case of accelerometric signals, the median filtering was applied to remove gross errors from observed sequences.

In the next step, the linear acceleration data without additional gravity components were processed. Their modulus $A_q(n)$ was evaluated from the components $Ax_q(n)$, $Ay_q(n)$, and $Az_q(n)$ recorded in three directions by relation

$$A_q(n) = \sqrt{Ax_q(n)^2 + Ay_q(n)^2 + Az_q(n)^2} \qquad (1)$$

for all values $n = 0, 1, 2, \cdots, N-1$ in each experiment $q = 1, 2, \cdots, Q$ of N values. In this way, the accelerometric values invariant to the rotation of the sensor during observations were evaluated.

The processing of multimodal records $\{d(n)\}_{n=0}^{N-1}$ of the accelerometric and heart rate signals was performed by similar numerical methods. After high-pass filtering removed the slowly varying signal components, short-time discrete Fourier transform was applied to detect the time-varying frequency parts.

Each accelerometric signal $\{d(n)\}_{n=0}^{N-1}$ of N samples that was observed during each experiment was processed in time windows $TW = 30$ s long to evaluate the associated signal spectrum, covering the full frequency range of $\langle 0, f_s/2\rangle$ Hz for $f_s = 1/T_s$. This method was used to evaluate the spectrogram for each experiment. The accelerometric signal and its spectrogram are presented in Figs. 1(c,d) for a selected cycling experiment.

The following two frequency bands were then selected for evaluation of accelerometric features:

- Range $r_1 = \langle f_{c1}, f_{c2}\rangle$,
- Range $r_2 = \langle f_{c3}, f_{c4}\rangle$.

for cutoff frequencies $f_{c1}, f_{c2}, f_{c3}, f_{c4}$ less than $f_s/2$. The relative power $p(i,j)$ in each frequency range r_1 and r_2 was then estimated by the relation

$$p(i,j) = \frac{\sum_{k\in\Phi_i} |D_j(k)|^2}{\sum_{k=0}^{N/2} |D_j(k)|^2}, \quad D_j(k) = \sum_{n=0}^{N-1} d_j(n)\, e^{-j\,kn\frac{2\pi}{N}} \qquad (2)$$

where Φ_i is the set of indices for the range of frequencies $f_k \in r_i$, $i = 1, 2$, and $j = 1, 2, \cdots, Q$ for the total number of experiments Q. This method was used to define the pattern matrix $\mathbf{P}_{2,Q}$. The locations of these features in the 2D domain for a selected experiment are presented in Fig. 3(d).

This article has been accepted for publication in a future issue of this journal, but has not been fully edited. Content may change prior to final publication. Citation information: DOI 10.1109/ACCESS.2021.3111323, IEEE Access

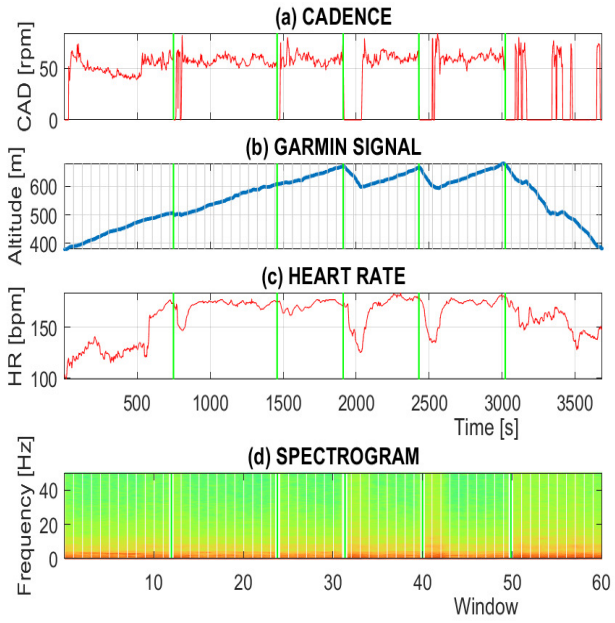

FIGURE 4. Time synchronisation of observed signals presenting (a) the cadence signal, (b) the Garmin altitude signal, (c) heart rate signal, and (d) spectrogram evaluated from the accelerometric signal recorded during the cycling route.

The Kohonen learning rule was then applied during the unsupervised learning process for data clustering to evaluate the network model later used to classify these features. The results of this clustering process with a one-layer neural network for a selected cycling experiment are presented in Figs. 3(c,d). The outputs from two neurons suggest separate signal classes.

The cadence cycling signal was then used to synchronise the separate signals. This approach was based on the assumption that this signal drops to zero on the top of each hill; as presented in Fig. 4(a), which corresponds with the route altitude profile in Fig. 4(b). This simple segmentation process enabled the evaluation of the signal features in each downhill route segment. A polynomial approximation of the signals in these cycling segments was then applied.

The spectrograms of accelerometric signals were then examined to classify the motion patterns using the selected neural network model. The supervised learning process was applied to classify the frequency components in time windows of the selected length. Time synchronisation of the signals and GNSS data enabled to the expected target values for the model's construction to be specified.

Results obtained after the chosen number of training epochs were then evaluated by the receiver operating characteristic (ROC). The machine learning process finds the number of true-negative (TN), false-positive (FP), true-positive (TP) and false-negative (FN) values in the negative set (class 1: downhill cycling) and positive set (class 2: uphill cycling). The associated performance metrics can then be used to evaluate:

- The true positive rate (TPR, sensitivity), the true negative rate (TNR, specificity), the false negative rate (FNR), and the false positive rate (FPR)

$$TPR = \frac{TP}{TP+FN}, \quad TNR = \frac{TN}{TN+FP} \tag{3}$$

$$FNR = \frac{FN}{TP+FN}, \quad FPR = \frac{FP}{TN+FP} \tag{4}$$

- The negative predictive value (NPV), the positive predictive value (PPV, precision), and the accuracy (ACC)

$$NPV = \frac{TN}{TN+FN}, \quad PPV = \frac{TP}{TP+FP} \tag{5}$$

$$ACC = \frac{TP+TN}{TP+TN+FP+FN} \tag{6}$$

The confusion matrices of the training and testing sets were then used as measures of the generalisation abilities of the classification model.

III. RESULTS

Analysis of the cycling experiments includes 26 cycling routes and 933 segments in the same hilly area which are all about 12 km long, as presented in Fig. 1. All of the evaluations were done in the MATLAB 2021a computational system. All of the longitude and latitude positioning data recorded during each cycling experiment by the satellite navigation network were projected into the geographical environment with the associated visualisation using the following MATLAB commands:

```
>> geoplot([Latitude],[Longitude],'.r')
>> geolimits([49.34 49.38],...
>>           [17.98 18.05])
>> geobasemap satellite
```

The red dots point to the route and the selection of the satellite geographical base map.

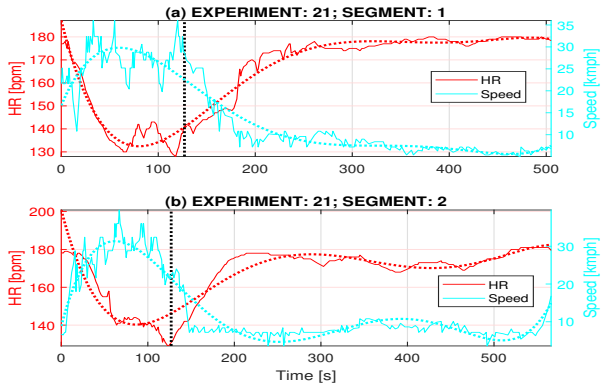

FIGURE 5. The polynomial approximation of the heart rate and the speed during a selected cycling experiment in (a) segment 1 and (b) segment 2 with the dash line separating downcycling and upcycling specified by the cadence sensor.

This article has been accepted for publication in a future issue of this journal, but has not been fully edited. Content may change prior to final publication. Citation information: DOI 10.1109/ACCESS.2021.3111323, IEEE Access

Fig. 5 presents the polynomial approximation of the fifth order applied to the heart rate and the speed during a selected cycling experiment in two route segments, with their initial points specified by the first and the second peak of the cycling route. Complete results for all experiments are presented in Fig. 6. Starting times are defined by the cadence signal and the length of the downhill cycling is projected from the altitude GPS signal. For a selected experiment, the heart rate, the speed, and the relative accelerometric power in the frequency band of $\langle 30, 40 \rangle$ Hz are emphasised in individual subplots.

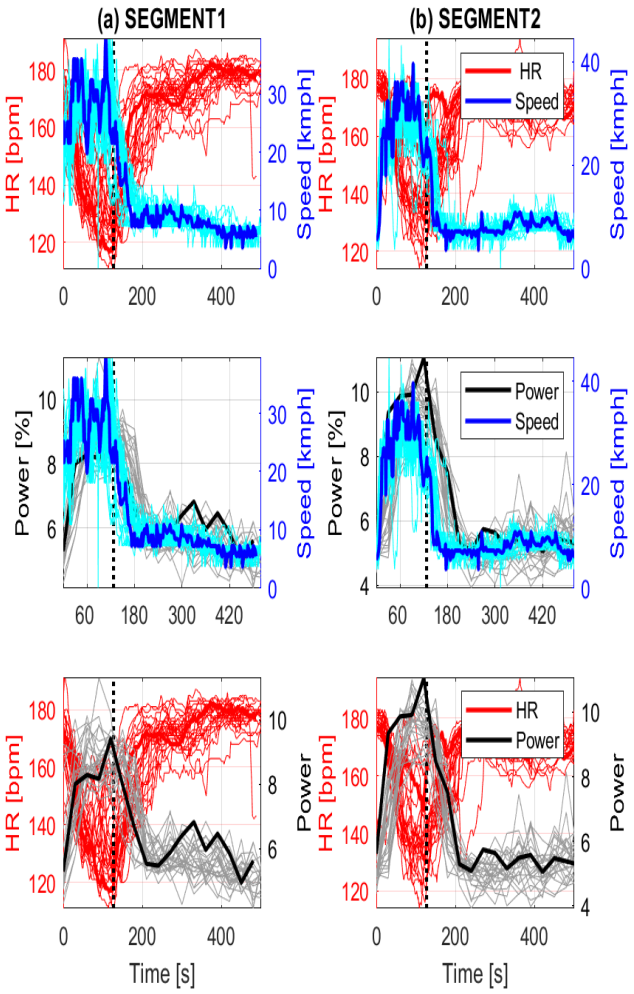

FIGURE 6. Comparison of the heart rate vs. speed, the relative mean power of the accelerometric signal in the frequency range $\langle 30, 40 \rangle$ Hz vs. speed, and the heart rate vs. the relative mean power in the frequency range $\langle 30, 40 \rangle$ Hz for 26 cycling experiments and the dash line separating downcycling and upcycling specified by the cadence sensor.

IV. DISCUSSION

The signals presented in Fig. 6 were used to evaluate the correspondence between selected signals and to eliminate any experiments with gross errors. The processing of each experiment included the polynomial approximation to each record and the evaluation of the delay between separate signals for a 50 % decrease of the heart rate after the cadence change. The difference between these peak values outside the given range excluded 9.9 % of experiments. A summary of all of the results is presented in Table 1, with similar results in both segments. The mean delay of the heart rate change and acceleration change was 20.6 s in the given conditions. The relative accelerometric power was evaluated in the frequency band of $\langle 30, 40 \rangle$ Hz and 933 time windows 30 s long were used for the following classification.

TABLE 1. Comparison of delays and standard deviations (STD) of selected variables recorded during cycling for two selected cycling segments and the set of cycling routes for Heart Rate vs Speed (*HRS*), Power vs Speed (*PWS*), Heart rate vs Power (*HRPW*), and Heart Rate vs Cadence Change (*HRC*).

Comparison	*Segment 1*		*Segment 2*	
	Delay [s]	*STD*	*Delay [s]*	*STD*
HRS	29.2	11.6	33.9	15.7
PWS	16.6	9.0	10.8	6.1
HRPW	17.7	11.7	23.4	15.6
HRC	20.2	5.3	25.2	8.7

Results indicate an average value of 22.7 s for the heart rate to decrease by 50 % between its highest and lowest value resulting from the cadence change. This result corresponds with experiments on the exercise bike [25] for a healthy person. The heart rate recovery delay is considered to be an indicator of physical and nervous condition [44].

Figure 7 presents the results of the classification of the spectral features of the accelerometric data into two classes

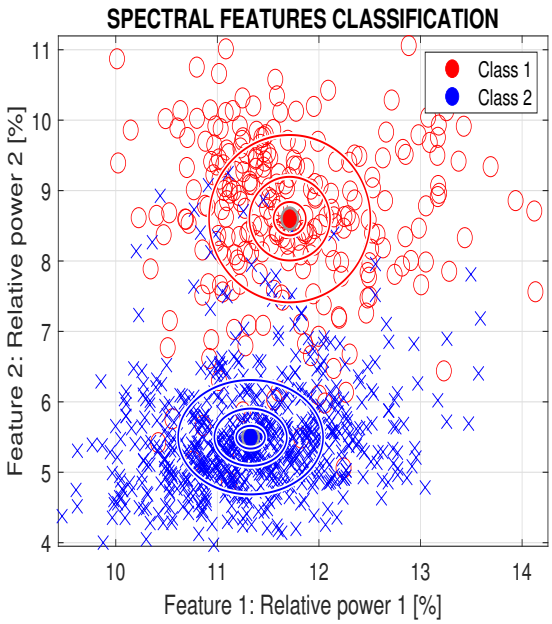

FIGURE 7. Classification of spectrogram features related to accelerometric data of all experiments using the relative mean power in selected frequency ranges ($F1 : \langle 10, 15 \rangle$ Hz and $F2 : \langle 30, 40 \rangle$ Hz) presenting segments belonging to class 1 (downhill cycling) and class 2 (uphill cycling) using the two layer neural network with centers of gravity of individual classes and c-multiples of standard deviations for $c = 0.2, 0.5, 1$.

This article has been accepted for publication in a future issue of this journal, but has not been fully edited. Content may change prior to final publication. Citation information: DOI 10.1109/ACCESS.2021.3111323, IEEE Access

(class 1: downhill cycling, class 2: uphill cycling) using the two layer neural network with 10 elements in the first layer for the whole set of cycling experiments. The features were defined as the relative mean power in selected frequency ranges ($F1 : \langle 10, 15 \rangle$ Hz and $F2 : \langle 30, 40 \rangle$ Hz). The optimisation process was applied for a standard neural network with 10 neurons in the first layer that included the sigmoidal transfer function and 2 elements in the second softmax layer. Figure 7 also presents the centers of gravity of the individual classes and c-multiples of standard deviations for $c = 0.2, 0.5, 1$.

The confusion matrix for the training and testing sets is presented in Table 2. The accuracy achieved was 93.9 % and 95.0 % for the training and testing sets, respectively.

TABLE 2. Confusion matrix of the classification by the two layer neural network model for the training and testing sets with true positive values on the matrix diagonal (in the bold), true positive/negative rates $TR(k)$, and positive/negative prediction values $PV(k)$.

Precision Colorbar									
82	84	86	88	90	92	94	96	98	100

(a) CONFUSION MATRIX / Train Set

	Class	*Target*		$PV(k)$
	k	Class 1	Class 2	
Output	Class 1	**166**	15	89.7
	Class 2	21	**447**	95.5
$TR(k)$		88.8	95.9	**ACC: 93.9**

(b) CONFUSION MATRIX / Test Set

	Class	*Target*		$PV(k)$
	k	Class 1	Class 2	
Output	Class 1	**31**	4	88.6
	Class 2	3	**102**	97.1
$TR(k)$		92.2	96.2	**ACC: 95.0**

The supplementary material includes the animation of signals recorded during a selected cycling segment and their processing.

V. CONCLUSION

This paper has presented the use of selected wearable sensors and appropriate computational method for the assessment of physical activities and motion monitoring during cycling in real conditions. Positioning data recorded by the GNSS system, heart rate data, cycling cadence-derived data, and accelerometric data recorded by a sensor in the mobile phone were used to detect a number of motion patterns. Using the event data records, the paper helps cyclists to analyse cycling-related information.

A new methodology is presented in which cycling cadence and time stamps are used, allowing accurate segmentation and synchronization of signals recorded by different wearable sensors. The paper moreover presents results which indicate the heart rate recovery delay after a cadence change, with motion patterns successfully derived from accelerometric signals in real conditions. The results suggest that cycling cadence, accelerometric, and heart rate data can be used to evaluate and recognise motion patterns during cycling in different route conditions. The observed mean delay of the change of the heart rate that was related to the change of the mean power of the accelerometric signal in the high-frequency band was 20.6 s for the given set of experiments in real conditions and hilly route areas.

The proposed methodology was based on the Kohonen learning rule and a softmax neural network structure. Our future work will be devoted to the use of more sophisticated models and a deep learning strategy. Applications will be developed using a similar methodology to characterise motion in different sports activities including running and skiing with a modified approach to the synchronization of signals from different sensors. Particular attention also will be paid to medical applications where advances may be expected in the detection of neurological disorders, ataxic gate monitoring, and rehabilitation, through motion pattern analysis.

REFERENCES

[1] P. Silsupadol, K. Teja, and V. Lugade. Reliability and validity of a smartphone-based assessment of gait parameters across walking speed and smartphone locations: Body, bag, belt, hand, and pocket. Gait Posture, 58:516–522, 2017.

[2] A. Procházka, O. Vyšata, M. Vališ, O. Ťupa, M. Schatz, and V. Mařík. Bayesian classification and analysis of gait disorders using image and depth sensors of Microsoft Kinect. Digit. Signal Prog., 47(12):169–177, 2015.

[3] P.D. Loprinzi and B. Smith. Comparison between wrist-worn and waist-worn accelerometry. J. Phys. Act. Health, 14(7):539–545, 2017.

[4] K.A. Mackintosh, A.H.K. Montoye, K.A. Pfeiffer, and M.A. McNarry. Investigating optimal accelerometer placement for energy expenditure prediction in children using a machine learning approach. Physiol. Meas., 37(10):1728–1740, 2016.

[5] A. Procházka, M. Schätz, F. Centonze, J. Kuchyňka, O. Vyšata, and M. Vališ. Extraction of Breathing Features Using MS Kinect for Sleep Stage Detection. Signal Image Video Process., 10(7):1278–1286, 2016.

[6] A.L. Ridgel, H.M. Abdar, J.L. Alberts, F.M. Discenzo, and K.A. Loparo. Variability in cadence during forced cycling predicts motor improvement in individuals with parkinson's disease. IEEE Trans. Neural Syst. Rehabil. Eng., 21(3):481–489, 2013.

[7] L.A. Leyland, B. Spencer, N. Beale, T. Jones, and C.A. van Reekum. The effect of cycling on cognitive function and well-being in older adults. Plos one, 20:1–17, 2019.

[8] G.M. Weiss, K. Yoneda, and T. Hayajneh. Smartphone and Smartwatch-Based Biometrics Using Activities of Daily Living. IEEE Access, 7:133190–133202, 2019.

[9] B. Cvetkovic, R. Szeklicki, V. Janko, P. Lutomski, and M. Luštrek. Real-time activity monitoring with a wristband and a smartphone. Inf. Fusion, 43:77 – 93, 2018.

[10] A. Mannini, M. Rosenberger, W.L. Haskell, A.M. Sabatini, and S.S. Intille. Activity recognition in youth using single accelerometer placed at wrist or ankle. Med. Sci. Sports Exerc., 49(4):801–812, 2017.

[11] M.H. Haider, A. Tabassum, R.H. Shihab, and C.M. Hasan. Comparative analysis of GNSS reliability: GPS, GALILEO and combined GPS-GALILEO. In 1st International Conference on Electrical Information and Communication Technology, pages 1–6, Feb 2014.

[12] S. Lissner and S. Huber. Facing the needs for clean bicycle data – a bicycle-specific approach of GPS data processing. European Transport Research Review, 13(8):1–14, 2021.

[13] A.B. Cooke, S.S. Daskalopoulou, and K. Dasgupta. The impact of accelerometer wear location on the relationship between step counts and arterial stiffness in adults treated for hypertension and diabetes. J. Sci. Med. Sport, 21(4):398–403, 2018.

[14] A. Procházka, O. Vyšata, H. Charvátová, and M. Vališ. Motion Symmetry Evaluation Using Accelerometers and Energy Distribution. MDPI: Symmetry, 11:2929:1–2929:13, 2019.

[15] J.J. Guiry, P. van de Ven, J. Nelson, L. Warmerdam, and H. Ripe. Activity recognition with smartphone support. Med. Eng. Phys., 36(6):670 – 675, 2014.

[16] R. Gajda, E. K. Biernacka, and W. Drygas. Are heart rate monitors valuable tools for diagnosing arrhythmias in endurance athletes? Scandinavian Journal of Medicine, 28(2), 2018.

[17] M.A. Wister, P. Pancardo, R.H. Shihab, and P.P. Campos. A Comparative Study of Cycling Mobile Applications. In The 3rd International Conference on Smart and Sustainable Technologies (SpliTech), pages 1–4, June 2018.

[18] J. Wannenburg and R. Malekian. Physical Activity Recognition From Smartphone Accelerometer Data for User Context Awareness Sensing. IEEE Trans. Syst. Man Cybern. Syst., 47(12):3142–3149, Dec 2017.

[19] H. Monkaresi, R. A. Calvo, and H. Yan. A Machine Learning Approach to Improve Contactless Heart Rate Monitoring Using a Webcam. IEEE J. Biomedical Health Informat., 18(4):1153–1160, 2014.

[20] A. Procházka, H. Charvátová, O. Vyšata, J. Kopal, and J. Chambers. Breathing Analysis Using Thermal and Depth Imaging Camera Video Records. Sensors (Basel, Switzerland), 17:1408:1–1408:10, 2017.

[21] A.H. Alkali, R. Saatchi, H. Elphick, and D. Burke. Thermal image processing for real-time non-contact respiration rate monitoring. IET Circuits Devices Syst., 11(2):142–148, 2017.

[22] J. Ruminski. Analysis of the parameters of respiration patterns extracted from thermal image sequences. Biocybern. Biomed. Eng., 36(4):731–741, 2016.

[23] M. Ambrosanio, S. Franceschini, G. Grassini, and F. Baselice. A multichannel ultrasound system for non-contact heart rate monitoring. IEEE Sensors J., 20(4):2064–2074, 2020.

[24] K. Zang, J. Shen, H. Huang, M. Wan, and J. Shi. Assessing and Mapping of Road Surface Roughness based on GPS and Accelerometer Sensors on Bicycle-Mounted Smartphones. Sensors (Basel, Switzerland), 18:914:1–914:17, 2018.

[25] O. Dostál, A. Procházka, O. Vyšata, O. Ťupa, P. Cejnar, and M. Vališ. Recognition of Motion Patterns Using Accelerometers for Ataxic Gait Assessment. Neural Computing and Applications, 33:2207–2215, 2021.

[26] A. Procházka, O. Dostál, P. Cejnar, H.I. Mohamed, Z. Pavelek, M. Vališ, and O. Vyšata. Deep Learning for Accelerometric Data Assessment and Ataxic Gait Monitoring. IEEE Transaction on Neural Systems and Rehabilitation Engineering, 29:33434133:1–33434133:8, 2021.

[27] A. Procházka, Charvátová. H., O. Vyšata, D. Jarchi, and S. Saeid. Discrimination of Cycling Patterns Using Accelerometric Data and Deep Learning Techniques. Neural Computing and Applications, xx(x):1–11, 2020.

[28] M.T. Sadiq, X. Yu, Z. Yuan, F. Zeming, S. Rehman, A.U., I. Ullah, G. Li, and G. Xiao. Motor Imagery EEG Signals Decoding by Multivariate Empirical Wavelet Transform-Based Framework for Robust Brain-Computer Interfaces. IEEE Access, 7:171431–171451, 2019.

[29] M.T. Sadiq, X. Yu, and Z. Yuan. Exploiting dimensionality reduction and neural network techniques for the development of expert brain–computer interfaces. Expert Systems with Applications, 164:114031:1–20, 2021.

[30] H. Cho and Yoon S.M. Applying singular value decomposition on accelerometer data for 1D convolutional neural network based fall detection. Electronics Letters, 55(6):320–322, 2019.

[31] M.T. Sadiq, X. Yu, Z. Yuan, M.Z. Azis, S. Siuly, and W. Ding. Towards the Development of Versatile Brain-Computer Interfaces. Journal of IEEE Transactions on Artificial Intelligence, pages 1–1, 2021.

[32] A. Procházka, S. Vaseghi, M. Yadollahi, O. Ťupa, J. Mareš, and O. Vyšata. Remote Physiological and GPS Data Processing in Evaluation of Physical Activities. Med. Biol. Eng. Comput., 52:301–308, 2014.

[33] H. Charvátová, A. Procházka, S. Vaseghi, O. Vyšata, and M. Vališ. GPS-based Analysis of Physical Activities Using Positioning and Heart Rate Cycling Data. Signal Image Video Process., 11(6):251–258, 2017.

[34] Y.X. Zhao, Y.S. Su, and Y.C. Chang. A Real-Time Bicycle Record System of Ground Conditions Based on Internet of Things. IEEE Access, 5:17525–17533, 2017.

[35] A. Procházka, S. Vaseghi, H. Charvátová, O. Ťupa, and O. Vyšata. Cycling Segments Multimodal Analysis and Classification Using Neural Networks. Appl. Sci., 7:581:1–581:11, 2017.

[36] A. Procházka, H. Charvátová, S. Vaseghi, and O. Vyšata. Machine Learning in Rehabilitation Assesment for Thermal and Heart Rate Data Processing. IEEE Trans. Neural Syst. Rehabil. Eng., 26(6):1209–12141, 2018.

[37] A. Procházka, O. Vyšata, and V. Mařík. Integrating the Role of Computational Intelligence and Digital Signal Processing in Education. IEEE Signal Processing Magazine, 38(3):154–162, 2021.

[38] A. Dutta, O. Ma, M. Toledo, A.F. Pregonero, B.E. Ainsworth, M.P. Buman, and D.W. Bliss. Identifying free-living physical activities using lab-based models with wearable accelerometers. Sensors (Switzerland), 18(11), 2018.

[39] R. Ganea, A. Paraschiv-Lonescu, and K. Aminian. Detection and classification of postural transitions in real-world conditions. IEEE Trans. Neural Syst. Rehabil. Eng., 20(5):688–696, 2012.

[40] S.A. Evans, D.A. James, D. Rowlands, and J.B. Lee. Evaluation of Accelerometer-Derived Data in the Context of Cycling Cadence and Saddle Height Changes in Triathlon. Sensors, 21:871:1–871:13, 2021.

[41] A. Procházka, O. Dostál, P. Cejnar, H.I. Mohamed, Z. Pavelek, M. Vališ, and O. Vyšata. Deep Learning for Accelerometric Data Assessment and Ataxic Gait Monitoring. IEEE Transaction on Neural Systems and Rehabilitation Engineering, 29:33434133:1–8, 2021.

[42] S.D. Din, A. Hickey, N. Hurwitz, J.C. Mathers, L. Rochester, and A. Godfrey. Measuring gait with an accelerometer-based wearable: influence of device location, testing protocol and age. Physiol. Meas., 37:1785–1797, 2016.

[43] G.H. Goldsztein. Modeling walking with an inverted pendulum not constrained to the sagittal plane. numerical simulations and asymptotic expansions. Applied Mathematics, 8:57–76, 2017.

[44] J. Lou, W.R. Shi, Y. Dong, Y.P. Jin, and X.G. Guo. The impact of delayed heart rate recovery on prevalent hypertension. Postgraduate Medicine, 133(3):362–368, 2021.

HANA CHARVÁTOVÁ received a Ph.D. in 2007 in Chemistry and Materials Technology at the Faculty of Technology, TBU, Zlín for the Technology of Macromolecular Substances. Currently, she is associated with the Centre for Security, Information and Advanced Technologies (CEBIA – Tech), Faculty of Applied Informatics, TBU, Zlín. Her research interests include modelling manufacturing processes of natural and synthetic polymers, analysis of thermal processes in building technology, studies of sensor system and wireless communication, signal processing for motion monitoring, and modelling of engineering and information systems. She is oriented towards computational and visualisation methods in thermographics, spatial modelling, and engineering. She serves as a reviewer for Springer, Elsevier, Wiley, Taylor and Francis, and MDPI journals.

ALEŠ PROCHÁZKA (Life Member, IEEE) received a Ph.D. in 1983 and was appointed Professor in Technical Cybernetics by the Czech Technical University in 2000. He is the Head of the Digital Signal and Image Processing Research Group at the Department of Computing and Control Engineering, UCT, Czech Institute of Informatics, Robotics and Cybernetics, CTU, Prague, and a member of IEEE, IET and EURASIP scientific societies. His research interests include mathematical methods of multidimensional data analysis, segmentation, feature extraction, classification, and modelling in biomedicine and engineering. He has served as an Associate Editor for Springer Signal, Image and Video Processing Journal, and he is a reviewer for different IEEE Transactions and Springer, Elsevier and MDPI journals.

This article has been accepted for publication in a future issue of this journal, but has not been fully edited. Content may change prior to final publication. Citation information: DOI 10.1109/ACCESS.2021.3111323, IEEE Access

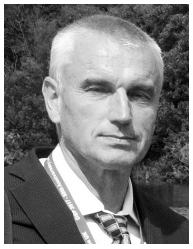

OLDŘICH VYŠATA (IEEE Member) received the MD in 1985 and a Ph.D. in Technical Cybernetics at the Institute of Chemical Technology in Prague, Czech Republic in 2011. He is a member of the Digital Signal and Image Processing Research Group at the Department of Computing and Control Engineering, UCT, Prague, the European Neurological Society, the Czech Society of Clinical Neurophysiology, the Czech League against Epilepsy, and the Czech Medical Association of J. E. Purkyně. He is oriented towards computational medicine, analysis of motion disorders, and machine learning. Currently, he is associated with the Neurological department of the University Hospital of the Charles University in Hradec Kralove, Czech Republic, and he serves as a reviewer for different Springer, Elsevier, and MDPI journals.

CARMEN PAZ SUÁREZ-ARAUJO (IEEE Member) received a MS in Physics and a Ph.D. in Computer Sciences. She is the Head of the Computational Neuroscience Research Division at the Institute of Cybernetics Science and Technology of the ULPGC and of the Intelligent Computing, Perception and Big Data Research Group of ULPGC. Her research work is focused in natural and artificial neural networks, design of new neural architectures, application of neural computing in clinical, biomedical, environmental domains, computational neuroscience and cognitive computation, intelligent computing for translational and personalized medicine (non-communicable diseases associated with ageing). She serves as a reviewer of Springer, Elsevier, IEEE, Oxford Academic, World Scientific, Wiley, Plos-One, among others and an evaluator of international and national Evaluation Agencies.

JONATHAN HURNDALL SMITH received a Ph.D. in 1990 from Cambridge University Engineering department. He has held teaching positions at the Czech Technical University, South Bank University in London, and the International University in Ho Chi Minh. He is a member of the Institute of Physics (InstP) and Chartered Physicist (CPhys). He is currently director of Bellford Consultancy Services and conducts consultancy activities in Fibre Optic networks. His research interests include numerical and computational methods of multidimensional signal processing, functional transforms, telecommunications, cyber-physical systems, and applications in vibration analysis, photovoltaic energy production, submarine networks, and optical systems modelling.